ChemComm

Accepted Manuscript

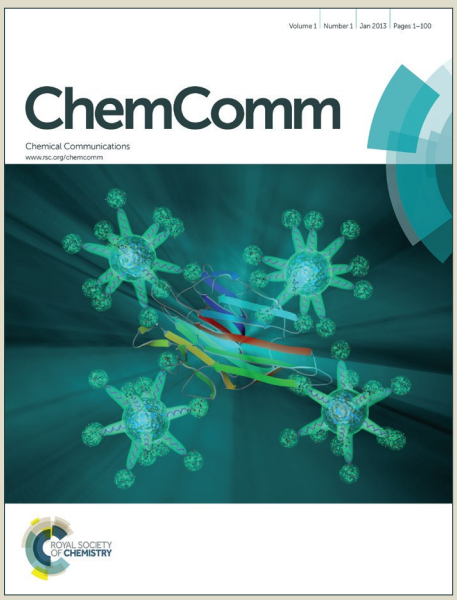

ROYAL SOCIETY OF CHEMISTRY

www.rsc.org/chemcomm

Cite this: DOI: 10.1039/c0xx00000x

www.rsc.org/xxxxxx

ARTICLE TYPE

A Mitochondria-Targetable Fluorescent Probe for Peroxynitrite: Fast Response and High Selectivity

Hongxing Zhang,[‡a] Jing Liu,[‡a] Yuan-Qiang Sun,[a] Yingying Huo,[a] Yaohua Li,[a] Weizhi Liu,[a] Xiao Wu,[a] Nishu Zhu,[a] Yawei Shi,[b] and Wei Guo*[a]

Received (in XXX, XXX) Xth XXXXXXXXX 20XX, Accepted Xth XXXXXXXXX 20XX

DOI: 10.1039/b000000x

A mitochondria-targetable fluorescence probe, methyl(4-hydroxyphenyl)amino-substituted pyronin (1), was exploited, which could highly selectively sense peroxynitrite ($ONOO^-$) within seconds.

Peroxynitrite ($ONOO^-$), a powerful oxidizing and nitrating agent in living systems, is formed by reaction between nitric oxide (NO) and superoxide ($O_2^{\bullet-}$) under diffusion control without the need of enzymatic catalysis.[1] $ONOO^-$ can react with a wide array of biomolecules, such as proteins, lipids, and nucleic acids, resulting in cell death. As a result, $ONOO^-$ has been implicated in a variety of disease states, including Alzheimer's disease, arthritis, cancer, autoimmune and inflammatory disease, and other disorders.[2] However, evidences also revealed that $ONOO^-$ plays a positive role in either signal transduction via nitrating tyrosine residues[3] or immunogenic response against invading pathogens.[4] Therefore, methods for detection of cellular $ONOO^-$ levels are of considerable importance for both disease diagnosis and exploration of its various pathophysiology. However, due to its very short lifetime (~10 ms),[2d] low steady-state concentration (nM range)[5] as well as the potential interference from other reactive oxidative species (ROS), sensitively and selectively probing the biologically important species in biological systems has been a focal point. In addition, mitochondria is the main organelle where NO is synthesized by inducible NO synthase (iNOS); moreover, mitochondrial electron leak is a main pathway to produce $O_2^{\bullet-}$ via NADPH oxidase. As such, mitochondrial has been recognized to be the major site for the formation and reaction of intracellular $ONOO^-$.[2,6] Obviously, the detection of mitochondria $ONOO^-$ would be even more significant for better understanding of its origins, activities, and biological functions.

Fluorescent probes have been recognized as the most efficient molecular tools for detecting and imaging trace amounts of biomolecules in biological systems due to the simplicity, sensitivity, and real-time and nondestructive detection. The early stage fluorescent probes for $ONOO^-$ are based on the reduced nonfluorescent rhodamine or fluorescein dyes, which can be converted to fluorescent products upon being oxidized by $ONOO^-$.[7] However, these probes have little selectivity among various ROS. Afterwards, a number of small-molecule fluorescent probes with the improved performance were exploited based on the $ONOO^-$-triggered specific reactions, including aromatic nitration,[8] formation of dioxirane with activated ketones,[9] oxidation of organoselenium/organotellurium[10] or phenol,[11] chemical transformation of boronate to phenol,[12] and formation and subsequent hydrolysis of nitrosamine.[13] However, considering the real-time determination of $ONOO^-$ in biological systems, the sensitive and especially fast response still remains challenging. Recently, studies have shown that the boronate-containing fluorescent probes[14] and a dansyl-based one[13] could detect $ONOO^-$ within 20 s. Noteworthy is that a *N*-phenylrhodol-based fluorescent probe was recently reported to be able to detect $ONOO^-$ with a faster response (less than 5 s) and a ultra-low detection limit (as low as 10 nM).[15] From the real-time detection of $ONOO^-$ point of view, these probes appear to be more advantageous for application in biological systems. However, the weakness, if anything, would be that some interferences caused by excess other ROS, particularly hypochlorite (ClO^-) and hydrogen peroxide (H_2O_2), were still observable especially in lengthened incubation time. This may be a problem to be solved because the steady-state concentration for intracellular $ONOO^-$ is estimated to be in the nanomolar range,[2a,5] while for intracellular ClO^- to be in the micromolar range.[16] In addition, although mitochondrial has been recognized to be the major site for formation and reaction of intracellular $ONOO^-$, as far as we know, only one mitochondria-targetable fluorescent probe for $ONOO^-$ was reported to date.[10b]

The above concerns encouraged us to develop the new fluorescent probe to sense $ONOO^-$ with not only the high selectivity and sensitivity, but also the mitochondria-targetable characteristic. Herein, we present a simple design strategy to construct a fluorescent probe for specific detection of $ONOO^-$ by the direct conjugation of a methyl(4-hydroxyphenyl)amino reaction group with a selected fluorophore. The design rationale is depicted in Fig. 1, and illustrated as follows. Methyl(4-hydroxyphenyl)amino was selected because the group was recently reported to be highly reactive to $ONOO^-$, but less efficient toward other ROS.[15] Moreover, the group was expected to be a good electron donor for photo-induced electron transfer (PET) due to its high electron density as well as the resulting high HOMO level. The electropositive pyronin was selected as fluorescence

reporter because the dye was expected to be targetable for mitochondria, just like the mitochondria-selective probes rhodamine 123 and tetramethylrosamine,[17] by electrostatic interaction due to the highly negative mitochondrial membrane potentials (about –180 mV).[18] We speculated that probe **1** is nonfluorescent due to the PET process from the methyl(4-hydroxyphenyl)amino group to the excited fluorophore, and upon two-electron oxidation of the electron-rich methyl(4-hydroxyphenyl)amino group by $ONOO^-$ and subsequent hydrolysis, a green-emissive aminopyronin[19] **2** would be generated *via* intermediate **M**,[15] thereby leading to the fluorescence off-on response for $ONOO^-$. In addition, the enhanced selectivity toward $ONOO^-$ over other ROS was also expected because the electropositive pyronin could partially decrease the electron density of methyl(4-hydroxyphenyl)amino group to resist oxidation. However, what remains uncertain is whether the enhanced selectivity would compromise the response time.

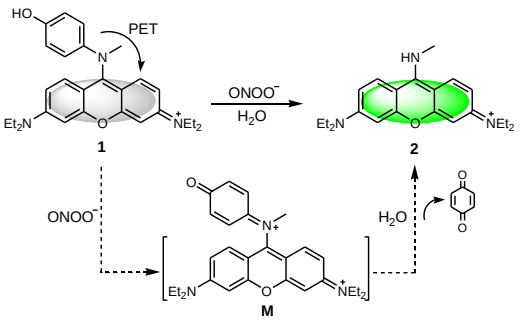

Fig. 1 Proposed sensing mechanisms of **1** for $ONOO^-$.

To test the above-mentioned speculation, we synthesized **1** by a simple procedure (ESI†). The structure of **1** was confirmed by ^1H NMR, ^{13}C NMR, and HRMS spectra. Subsequently, we examined the reactivity of **1** toward $ONOO^-$ in PB buffer (100 mM, pH 7.4) at 25 °C. As shown in Fig. S1 (ESI†), in the absence of $ONOO^-$, the solution of **1** (1 μM) showed a very poor fluorescence at 545 nm, indicating the efficient PET quenching process;[20] upon addition of $ONOO^-$ (8 μM) to the solution, a dramatic fluorescence enhancement (85-fold) was observed immediately. Notably, the time-dependent fluorescence intensity changes (at 545 nm) of **1** in the presence of $ONOO^-$ revealed that the reaction can be completed within seconds (Fig. 2A). In this regard, **1** is indeed superior to most of the reported $ONOO^-$ fluorescence probes[8-14] and comparable to HKGreen-4 reported recently.[15] Next we also tested the reactivity of **1** (1 μM) toward a series of ROS, including hypochlorite (ClO^-), hydroxyl radical ($^{\bullet}OH$), hydrogen peroxide (H_2O_2), superoxide ($O_2^{\bullet-}$), perborate (BO_3^-), nitrite (NO_2^-), nitric oxide (NO), and singlet oxygen ($^1O_2$), to evaluate the selectivity of the probe for $ONOO^-$. In fact, as shown in Fig. 2B (details in Fig. S2, ESI†), no changes in emission intensities occurred when the probe was incubated with 10 equiv of these ROS. Further, we tested the fluorescence response of **1** in the presence of more amounts of H_2O_2, ClO^-, and $^{\bullet}OH$ (100 μM), the main interferences in the detection of $ONOO^-$. Even in this case, only a 4-fold and a 2-fold fluorescence enhancements were observed for ClO^- and $^{\bullet}OH$, respectively, while no detectable change for H_2O_2 was found (Fig. S3, ESI†). Taken together, these results established that probe **1** is sensitive enough and also considerably selective toward $ONOO^-$ over other ROS.

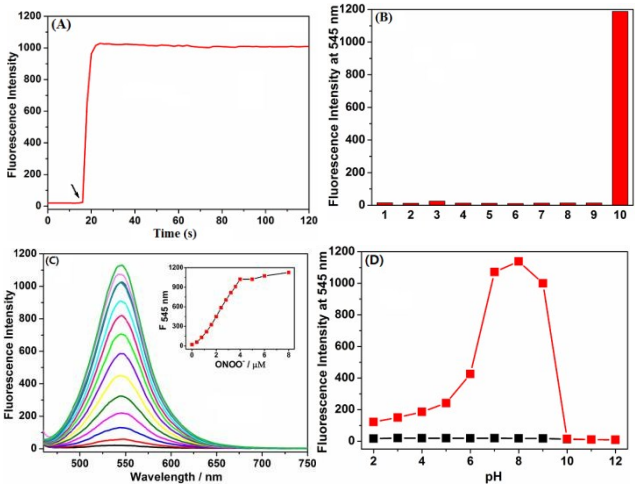

Fig. 2 (a) The time course of fluorescence intensity of **1** (1 μM) at 545 nm after adding 8 μM $ONOO^-$ in PB buffer (100 mM, pH 7.4) at 25 °C. (b) Fluorescence responses of **1** (1 μM) toward $ONOO^-$ and other ROS (all 10 μM) after 4 min. (1) **1** only; (2) ClO^-; (3) $^{\bullet}OH$; (4) H_2O_2; (5) $O_2^{\bullet-}$; (6) BO_3^-; (7) NO_2^-; (8) NO; (9) $^1O_2$; (10) $ONOO^-$. (c) Fluorescence spectra and intensity changes of **1** (1 μM) as a function of $ONOO^-$ concentrations (0–8 μM). (d) The fluorescence intensities at 545 nm of **1** (1 μM) in the absence and presence of $ONOO^-$ (10 μM) at varied pH values. λ_{ex} = 440 nm, λ_{em} = 545 nm. Slits: 5/10 nm, voltage: 600 V.

The fluorescence titration experiments for $ONOO^-$ were also performed in the same condition. As shown in Fig. 2C, upon treatment with the increasing concentrations of $ONOO^-$, the fluorescence intensity of **1** at 545 nm gradually increased, and when the amount of $ONOO^-$ was more than 4 equiv, the spectra saturation was reached. In this case, a linear calibration graph of the fluorescent intensities (I_{545}) to $ONOO^-$ concentrations from 0 μM to 4 μM was obtained (R^2 = 0.9959, Fig. S4, ESI†), and the detection limit was measured to be 4 nM based on S/N =3. In addition, the effect of pH on the fluorescence response of **1** to $ONOO^-$ was also tested (Fig. 2D). It was found that **1** was stable in a wide pH range of 2–12, and displayed the best response for $ONOO^-$ in the region of 7–9. Thus, probe **1** could function properly at physiological pH.

In order to probe the reaction mechanism, we subsequently tested the absorption spectra changes of probe **1** in the presence of $ONOO^-$ in the same condition. As shown in Fig. 3A, the free probe showed a main absorption at 510 nm; upon addition of $ONOO^-$, a new absorption peak at 440 nm emerged immediately. According to our proposed mechanism (Fig. 1), the new absorption peak could be assigned to aminopyronin **2**, which was supported by the same absorption and emission maxima of a synthetic sample **2** (Figs. 3B and 3C).[21] Moreover, TLC analysis of **1** treated with $ONOO^-$ displayed a new species that has the same Rf value and bright green fluorescence to those of **2** (Fig. S5, ESI†). Further, we performed HRMS experiment of probe **1** treated with $ONOO^-$, wherein the peak at *m*/*z* 352.2370 corresponding to product **2** was clearly observed (Fig. 3D).

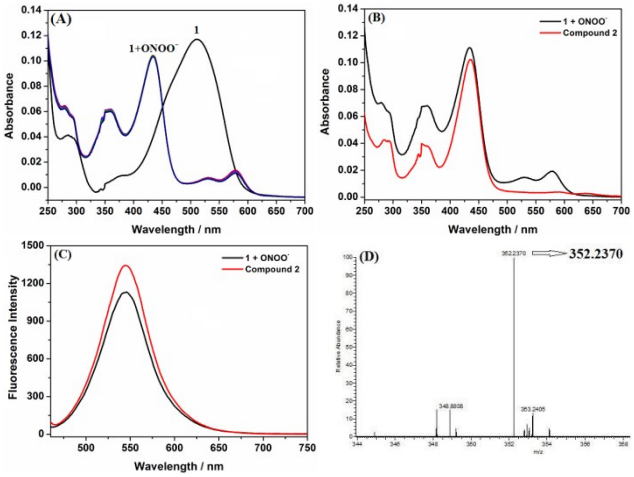

Fig. 3 (A) Absorption spectra of **1** (5 μM) upon addition of 100 equiv of $ONOO^-$. (B) Absorption spectra of **1** (5 μM) treated with 100 equiv of $ONOO^-$ *vs* that of product **2** (3 μM). (C) Fluorescence spectra of **1** (1 μM) treated with 8 equiv of $ONOO^-$ *vs* that of product **2** (0.5 μM). (D) HRMS chart of **1** in the presence of $ONOO^-$.

Subsequently, we evaluated the capability of probe **1** for the specific imaging of $ONOO^-$ in living cells (Fig. 4). The RAW264.7 murine macrophages were found to have almost no fluorescence when excited at 405 nm (Fig. 4A). When the cells were incubated with **1** (5 μM), they gave a slight fluorescence in green channel (Fig. 4B), suggesting that **1** may be sensitive to the low $ONOO^-$ level in the cells. When the **1**-loaded cells were treated with the $ONOO^-$ donor SIN-1 (3-morpholinosydnonimine),[22] strong fluorescence in green emission channel was observed (Fig. 4C). When the **1**-loaded cells were treated with either exogenous H_2O_2 or NaClO for 30 min, no noticeable fluorescence was observed (Figs. 4D and 4E). These results suggested that probe **1** has good cell permeability and could specifically image intracellular $ONOO^-$.

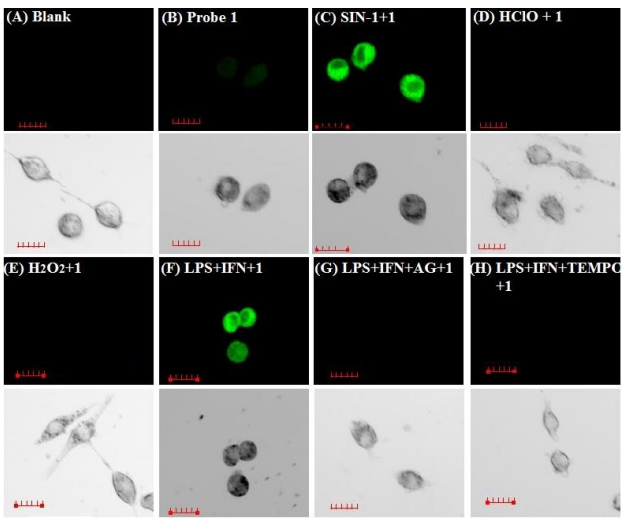

Fig. 4 Fluorescence images of **1**-loaded RAW264.7 murine macrophages under different conditions. (A) Blank; (B) cells were treated with **1** (5 μM, 30 min) and then imaged; (C) **1**-loaded cells were treated with SIN-1 (1 mM, 30 min) and then imaged; (D) **1**-loaded cells were treated with H_2O_2 (50 μM, 30 min) and then imaged; (E) **1**-loaded cells were treated with NaClO (50 μM, 30 min) and then imaged; (F) cells were stimulated with LPS (1 μg/mL) and IFN-γ (50 ng/mL) for 4 h and then with **1** (5 μM, 30 min); (G) NOS inhibitor AG (5 mM) was co-incubated during LPS (1 μg/mL)/IFN-γ (50 ng/mL) stimulation and then with **1** (5 μM, 30 min); (H) superoxide inhibitor TEMPO (300 μM) was co-incubated during LPS/IFN-γ stimulation and then with **1** (5 μM, 30 min). Quantification of fluorescence intensities of confocal microscopy images of RAW264.7 murine macrophages obtained under conditions A–H was shown in Fig. S6 (ESI†). Image from band path of 500-600 nm upon excitation of **1** at 405 nm. Scale bar: 20 μm.

Also, we performed fluorescence microscopic imaging of the endogenous $ONOO^-$ in activated RAW264.7 murine macrophages, which are known to produce $ONOO^-$ upon stimulation with interferon-γ (IFN-γ) and lipopolysaccharide (LPS).[23] As shown in Fig. 4F, when the cells were stimulated with IFN-γ/LPS and then treated with **1**, the dramatic fluorescence in green channel was observed. Moreover, when the cells were pretreated with the NO synthase inhibitor aminoguanidine (AG)[24] or superoxide scavenger 2,2,6,6-tetramethylpiperidine-N-oxyl (TEMPO)[25] during stimulation of the cells with IFN-γ/LPS, and then treated with probe **1**, almost no fluorescence within the cells could be observed (Figs. 4G and 4H). Thus, the strong green fluorescence from the activated RAW264.7 murine macrophages could be attributed to the formation of $ONOO^-$ and its rapid reaction with **1** to produce fluorescent **2**.

To confirm that probe **1** is a mitochondria-targetable probe for $ONOO^-$, bladder cancer BIU-87 cells were used in view of their larger size than RAW 264.7 cells. BIU-87 cells were treated in sequence with **1**, $ONOO^-$ donor SIN-1, and MitoTracker Red FM (a known fluorescence marker for mitochondria) in the culture media. After each treatment, the cells were washed with PBS 3 times. As shown in Figs. 5A1-A3, the green fluorescence signal was well-overlapped with the red fluorescence signal from the MitoTracker with a Pearson's coefficient of 0.86, indicating that the probe has good selectivity for mitochondria, and could specifically image mitochondrial $ONOO^-$ in the cells. To support the above result, a lysosome-localizing fluorescent dye (LysoTracker Red DND-99) and an endoplasmic reticulum-localizing fluorescent dye (ER-Tracker Red) were also used in the study. As shown in Figs. 5B1-B3 and Figs. 5C1-C3, no co-localization were essentially observed in both cases. In addition, the low cytotoxicity of **1** was also demonstrated by MTT assay (Fig. S7, ESI†).

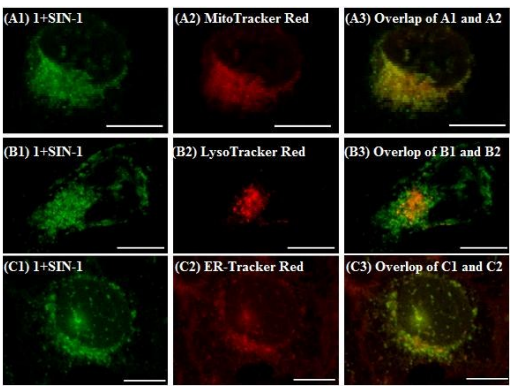

Fig. 5 (A1-A3) Fluorescence confocal images of BIU-87 cells costained by **1** (2 μM, 20 min), $ONOO^-$ donor SIN-1 (100 μM, 20 min), and then MitoTracker Red FM (0.2 μM, 30 min). (B1-B3) Fluorescence confocal images of BIU-87 cells costained by **1** (2 μM, 20 min), $ONOO^-$ donor

SIN-1 (100 μM, 20 min), and then LysoTracker Red DND-99 (50 nM, 30 min). (C1-C3) Fluorescence confocal images of BIU-87 cells costained by **1** (2 μM, 20 min), $ONOO^-$ donor SIN-1 (100 μM, 20 min), and then ER-Tracker Red (1.0 μM, 30 min). For A1, B1, and C1, images from band path of 460-530 nm upon excited at 405 nm. For A2, the excitation and emission bandpasses of the standard Cy5 filter set were used. For B2 and C2, the excitation and emission bandpasses of the standard TRITC filter set were used. (A3, B3, C3) The corresponding overlay images. Scale bar: 10 μm.

In summary, we presented a novel fluorescence probe **1** by the direct conjugation of a pyronin dye with a $ONOO^-$-sensitive methyl(4-hydroxyphenyl)amino reaction group. The probe was proved to be able to selectively and rapidly sense $ONOO^-$ over other ROS by $ONOO^-$-triggered oxidative N-dearylation reaction to release the fluorescent aminopyronin **2**. Assisted by laser scanning confocal microscope, we demonstrated that the probe is mitochondria-targetable, and could detect the exogenous and endogenous $ONOO^-$ in cells.

We acknowledge the Natural Science Foundation of China (Nos. 21172137 and 21302114) and Program for New Century Excellent Talents in University (NCET-11-1034) for support of this work.

Notes and references

[a] *School of Chemistry and Chemical Engineering, Shanxi University, Taiyuan 030006, China. E-mail: guow@sxu.edu.cn*
[b] *Institute of Biotechnology, Shanxi University, Taiyuan 030006, China.*

† Electronic Supplementary Information (ESI) available: Experimental procedures, supplemental spectra, and the ^1H–, ^{13}C– NMR, and MS spectrum. See DOI: 10.1039/b000000x/

‡ These authors contributed equally to this work.

1 R. Radi, *J. Biol. Chem.*, 2013, **288**, 26464.
2 (a) C. Szabó, H. Ischiropoulos, R. Radi, *Nat. Rev. Drug Discovery*, 2007, **6**, 662; (b) P. Pacher, J. S. Beckman, L. Liaudet, *Physiol. Rev.*, 2007, **87**, 315; (c) T. Nagano, *J. Clin. Biochem. Nutr.*, 2009, **45**, 111; (d) G. Ferrer-Sueta, R. Radi, *ACS Chem. Biol.*, 2009, **4**, 161.
3 L. Liaudet, G. Vassalli, P. Pacher, *Front Biosci.*, 2009, **14**, 4809.
4 (a) R. G. Allen, W. P. Lafuse, N. D. Powell, J. I. Webster Marketon, L. T. M. Stiner-Jones, J. F. Sheridan, M. T. Bailey, *Infect. Immun.*, 2012, **80**, 3429; (b) P. A. Darrah, M. K. Hondalus, Q. Chen, H. Ischiropoulos, D. M. Mosser, *Infect. Immun.*, 2000, **68**, 3387; (c) M. N. Alvarez, G. Peluffo, L. Piacenza, R. Radi, *J. Biol. Chem.*, 2011, **286**, 6627.
5 (a) N. Nalwaya, W. M. Deen, *Chem. Res. Toxicol.*, 2005, **18**, 486; (b) C. Quijano, N. Romero, R. Radi, *Free Radical Biol. Med.*, 2005, **39**, 728.
6 (a) R. Radi, A. Cassina, R. Hodara, C. Quijano, L. Castro, *Free Radical Biol. Med.*, 2002, **33**, 1451; (b) E. Nono, M. Parola, *Fibrog. Tissue Repair*, 2008, **1**, 5.
7 (a) H. Possel, H. Noack, W. Augustin, G. Keihoff, G. Wolf, *FEBS Lett.*, 1997, **416**, 175; (b) S. L. Hempel, G. R. Buettner, Y. Q. O'Malley, D. A. Wessels, D. M. Flaherty, *Free Radical Biol. Med.*, 1999, **27**, 146; (c) N. W. Kooy, J. A. Royall, H. Ischiropoulos, J. S. Beckman, *Free Radical Biol. Med.*, 1994, **16**, 149; (d) N. W. Kooy, J. A. Royall, H. Ischiropoulos, *Free Radical Res.*, 1997, **27**, 245; (e) I. Johnson and M. T. Z. Spence, The Molecular Probes Handbook: *A Guide to Fluorescent Probes and Labelling Technologies*, 2010.
8 T. Ueno, Y. Urano, H. Kojima, T. Nagano, *J. Am. Chem. Soc.*, 2006, **128**, 10640.
9 (a) D. Yang, H.-L. Wang, Z.-N. Sun, N.-W. Chung, J.-G. Shen, *J. Am. Chem. Soc.*, 2006, **128**, 6004; (b) Z.-N. Sun, H.-L. Wang, F.-Q. Liu, Y. Chen, P. K. Hang Tam, D. Yang, *Org. Lett.*, 2009, **11**, 1887; (c) T. Peng, D. Yang, *Org. Lett.*, 2010, **12**, 4932.
10 (a) F. Yu, P. Li, G. Li, G. Zhao, T. Chu, K. Han, *J. Am. Chem. Soc.*, 2011, **133**, 11030; (b) F. Yu, P. Li, B. Wang, K. Han, *J. Am. Chem. Soc.*, 2013, **135**, 7674.
11 Q. Zhang, Z. Zhu, Y. Zheng, J. Cheng, N. Zhang, Y.-T. Long, J. Zheng, X. Qian, Y. Yang, *J. Am. Chem. Soc.*, 2012, **134**, 17479.
12 (a) Z. Chen, W. Ren, Q. E. Wright, H. Ai, *J. Am. Chem. Soc.*, 2013, **135**, 14940; (b) J. Kim, J. Park, H. Lee, Y. Choi, Y. Kim, *Chem. Commun.*, 2014, **50**, 9353.
13 K.-K Lin, S.-C. Wu, K.-M. Hsu, C.-H. Hung, W.-F. Liaw, Y.-M. Wang, *Org. Lett.*, 2013, **15**, 4242.
14 (a) F. Yu, P. Song, P. Li, B. Wang, K. Han, *Analyst*, 2012, **137**, 3740. (b) J. Zhou, Y. Li, J. Shen, Q. Li, R. Wang, Y. Xu, X. Qian, *RSC Adv.*, 2014, **4**, 51589.
15 T. Peng, N.-K. Wong, X. Chen, Y.-K. Chan, D. H. Ho, Z. Sun, J. J. Hu, J. Shen, H. EI-Nezami, D. Yang, *J. Am. Chem. Soc.*, 2014, **136**, 11728.
16 M. R. McCall, A. C. Carr, T. M. Forte, B. Frei, *Arterioscl. Throm. Vas.*, 2001, **21**, 1040.
17 I. Johnson and M. T. Z. Spence, *The Molecular Probes Handbook—A Guide to Fluorescent Probes and Labeling Technologies*, Life Technologies, Carlsbad, Calif, USA, 11th edition, 2010.
18 (a) A. T. Hoye, J. E. Davoren, P. Wipf, M. P. Fink, V. E. Kagan, *Acc. Chem. Res.*, 2008, **41**, 87; (b) M. P. Murphy, R. A. J.Smith, *Annu. Rev. Pharmacol. Toxicol.*, 2007, **47**, 629.
19 L. Wu and K. Burgess, *Org. Lett.*, 2008, **10**, 1779.
20 We performed the viscosity experiments, and found that probe **1** is always nonfluorescent in the solutions with the variation of viscosity (EtOH-glycerol system) (Fig. S8, ESI†), thereby precluding the rotational relaxation mode of nonradiative decay due to the tertiary aniline unit.
21 The difference in absorption or fluorescent intensity between **1**+$ONOO^-$ and **2** is due to the unknown concentration of **2** produced by the reaction of **1** with $ONOO^-$.
22 N. Ashki, K. C. Hayes, F. Bao, *Neuroscience*, 2008, **156**, 107.
23 R. B. Lorsbach, W. J. Murphy, C. J. Lowenstein, S. H. Snyder and S. W. Russell, *J. Biol. Chem.*, 1993, **268**, 1908.
24 R. B. R. Muijsers, E. van den Worm, G. Folkerts, C. J. Beukelman, A. S. Koster, D. S. Postma and F. P. Nijkamp, *Br. J. Pharmacol.*, 2000, **130**, 932.
25 R. B. R. Muijsers, E. van den Worm, G. Folkerts, C. J. Beukelman, A. S. Koster, D. S. Postma, F. P. Nijkamp, *Br. J. Pharmacol.*, 2000, **130**, 932.